
Impact of inverter on losses and thermal characteristics of induction motors

Xiaofeng Ding

University of Michigan-Dearborn,
4901 Evergreen, Dearborn, MI 48128, USA
and
Northwestern Polytechnical University,
127 Youyi Xilu, Xi'an Shaanxi, 710072, China
E-mail: dxf_219@163.com

Chunting Chris Mi*

University of Michigan-Dearborn,
4901 Evergreen, Dearborn, MI 48128, USA
and
Northwestern Polytechnical University,
127 Youyi Xilu, Xi'an Shaanxi, 710072, China
E-mail: chrismi@umich.edu
*Corresponding author

Abstract: This paper investigated the losses and thermal characteristics of induction motors operated from pulse width-modulated (PWM) voltage supply in comparison to that operated from sinusoidal voltage supply. It was concluded that due to the abundant harmonics in the PWM waveforms, significant losses are induced in the motor by the inverter supply. The temperature ascends correspondingly. Switching frequencies of the PWM inverter at 3.5 kHz to 9 kHz were investigated to evaluate their effect on the excessive losses. Experiments were conducted with no load and with load conditions. The losses and thermal characteristics were calculated using finite-element analysis (FEA) and validated by the experiments.

Keywords: finite-element method; FEM; harmonics; pulse width-modulation; PWM; power electronics; frequency converter; induction machine; inverter; losses; thermal.

Reference to this paper should be made as follows: Ding, X. and Mi, C.C. (2011) 'Impact of inverter on losses and thermal characteristics of induction motors', *Int. J. Power Electronics*, Vol. 3, No. 6, pp.641–651.

Biographical notes: Xiaofeng Ding received his BSEE and his MSEE from Northwestern Polytechnical University, China, and is currently working towards his PhD at Northwestern Polytechnical University, China. He was an exchange student at the University of Michigan, Dearborn, Michigan, USA, from 2008 to 2010.

Chunting Chris Mi is Associate Professor of Electrical Engineering at the University of Michigan, Dearborn. He received his BSEE and his MSEE from Northwestern Polytechnical University, China, and his PhD from University of Toronto, Canada. His research interests are in power electronics, hybrid electric vehicles, electric machines and renewable energy systems. He worked for

General Electric Canada Inc. from 2000 to 2001. He is the recipient of numerous awards including the Distinguished Teaching Award and Distinguished Research Award from the University of Michigan, National Innovation Award and Government Special Allowance Award from China, and IEEE and SAE Awards. He is a senior member of IEEE and has more than 100 publications.

1 Introduction

The induction motor design requires a reliable estimation of the losses and corresponding temperature-rise, especially when the induction motor is driven by a pulse width-modulated (PWM) inverter (Uddin and Nam, 2008; Park et al., 2008; Bradley et al., 2008; Roshen, 2007; Yang et al., 2007). Inverter driven induction motors provide many advantages, such as wide speed range, and large torque capability over a wide speed range, etc. However, the abundant high frequency harmonics in the output voltage of the PWM inverter will induce additional losses (Liu et al., 2008; Khluabwannarat et al., 2007; Boglietti et al., 2010; Adley et al., 2008; Lee et al., 2004; Thammarat et al., 2005; Cao et al., 2010). These additional losses can be significant and are present in the stator winding, stator core, and rotor core. These losses further increase the temperature-rise within the induction machine (Mendes et al., 2008; Demetriades et al., 2010; Karagol and Bikdash, 2010). Consequently, the motor de-rates in performance. Therefore, the optimal design of an induction motor requires the consideration of thermal characteristics that provides improved efficiency and power density (Boglietti et al., 2002; Benhaddadi et al., 1997; Boglietti et al., 1994).

Previous studies have showed that the losses in an induction motor would increase when the motor is driven by PWM inverter. This paper performed a quantitative study on an induction motor. This paper investigates the losses and corresponding thermal characteristics of an induction motor driven by a sinusoidal and a PWM supply, respectively. The no load and loaded induction motor losses are first computed and analysed by using a time-stepped finite-element method (FEM). The losses of concern are copper losses in the windings and iron losses in the stator and rotor cores. The impact of the inverter on losses and thermal performance between the aforementioned two conditions is presented. Furthermore, switching frequencies of the PWM inverter are investigated to evaluate their effect on the losses. An equivalent thermal model was obtained including all the sources of losses in the motor. Using such a model the temperature profile of the motor is drawn from the FEM simulation. Experiments were carried out to validate the calculations on a 3 hp induction motor with a PWM inverter and a three-phase sinusoidal voltage source.

2 Harmonics in the PWM supply

PWM inverters are used widely to operate electrical motor. The rich harmonic contents in the output voltage of the PWM inverter induce additional losses in the motor. The bipolar PWM inverter induces more iron loss than unipolar PWM inverter (Khluabwannarat et al., 2007).

Figure 1 shows the basic principle of unipolar PWM. The output voltage can be written as follows (Halasz et al., 1996):

$$u = AU_d \sin(\omega_1 t + \varphi) + \sum_{V \neq 1}^{\infty} U_V \sin(v\omega_1 t + n\varphi) \quad (1)$$

where

$$U_V = \frac{2}{\pi K} U_d J_n \left(KA \frac{\pi}{2} \right) [(-1)^n - (-1)^K] \quad (2)$$

and

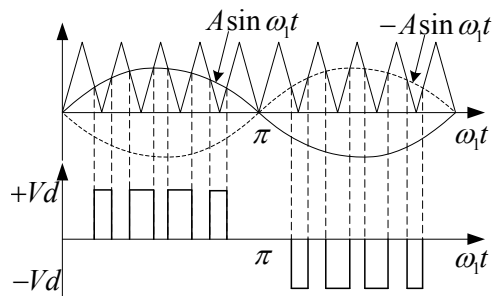
- $V = \pm Km + n > 0$ the order of harmonics
- ω_1 angular velocity of the fundamental component
- t time
- A amplitude of the reference wave ($A \leq 1$)
- $K = 2, 4, 6$ positive even integer
- $n = \pm 1, \pm 3, \pm 5$ positive or negative odd integer
- J_n first-kind Bessel function of the n order
- m ratio of the frequencies of the carrier and reference waves
- φ angle between the carrier and reference waves.

The output voltage of bipolar PWM contains the fundamental voltage, carrier frequency-related harmonics and other high frequency harmonic voltages. The general Fourier series of the output voltage is given as (Liu et al., 2008),

$$v(t) = \sum_{n=1}^{\infty} v_n(t) = \sum_{n=1}^{\infty} (a_n \cos n\omega t + b_n \sin n\omega t) = \sum_{n=1}^{\infty} V_n \sin(n\omega t + \varphi_n) \quad (3)$$

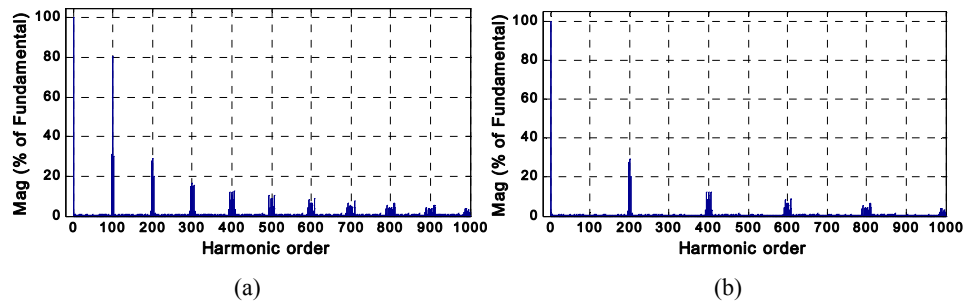
where ω is fundamental angular frequency, n is the order of harmonics, V_n is the amplitude of the n th harmonic, a_n and b_n are the Fourier coefficients, φ_n is the phase angle of the n th harmonic.

Figure 1 Unipolar PWM



The bipolar PWM output wave contains carrier frequency-related harmonics with modulation frequency-related sidebands represented as $mf_c + nf_1$, where m and n are integers and the sum of the integers is an odd integer, f_c is switch frequency and f_1 is reference wave frequency. Compared with bipolar PWM, equation (1) shows that unipolar modulation technique does not produce harmonics of the order Km (K is odd integer) or harmonics with orders $Km \pm n$ (K is odd integer). This results also can be apparently observed from Figure 2, which shows the harmonics spectrum of two PWM output voltages for $f_1 = 60$ Hz, $f_c = 6,000$ Hz and amplitude modulation ratio $M = 0.9$. Therefore, in this paper the unipolar PWM is used to drive the induction motor.

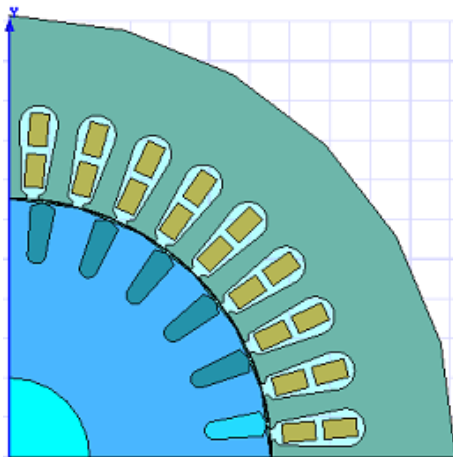
Figure 2 Harmonic spectrum of PWM waveforms, (a) bipolar PWM (b) unipolar PWM (see online version for colours)



3 Test motor and experiment bench

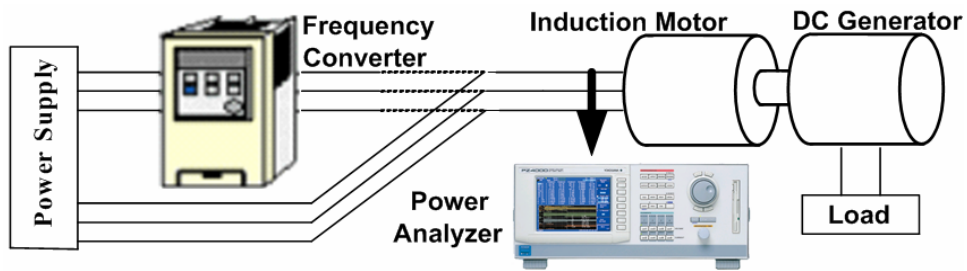
The experiment was carried out on a 3 hp induction motor. The motor is a four-pole, 60 Hz, 208 V, Y-connected, three-phase induction motor. Figure 3 shows the cross-section of the machine. The machine has a double layer three-phase stator winding, 36 slots in the stator and 24 slots in the rotor.

Figure 3 Experimental induction motor (see online version for colours)



The experiment bench is shown in Figure 4, which includes the power supply, a unipolar frequency converter, power analyser, induction motor, DC generator, and DC electronic load connected to the output of the DC generator. The solid line shows the induction motor is operated by the sinusoidal supply directly and the dotted line means the motor is driven by the PWM inverter. The power analyser is used to capture the line voltage and phase current.

Figure 4 Experiment bench (see online version for colours)

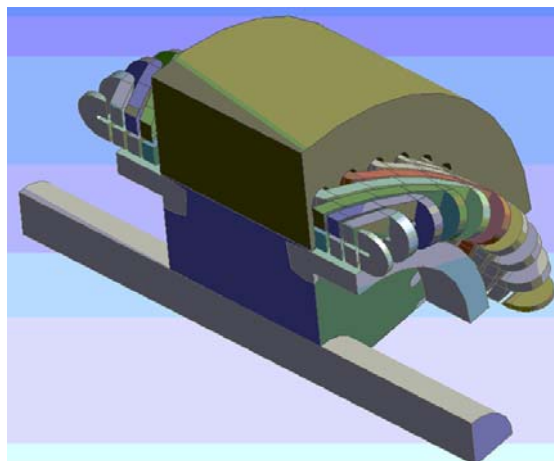


The input power of the induction motor can be obtained directly from the power analyser. Both no load and load tests were performed. Moreover, no load tests with a fundamental frequency of 60 Hz and switching frequency ranging from 3.5 kHz to 9 kHz were carried out to evaluate the influences of switching frequency on the additional losses.

4 Numerical simulation

To understand the mechanism of the additional losses, a two dimensional (2D) FEM was developed to compute the losses depicted in Figure 3. And a three-dimensional (3D) FEM model was also set up to estimate the thermal profile within the motor, as shown in Figure 5.

Figure 5 Thermal model (see online version for colours)



4.1 Sinusoidal supply

The values of the sinusoidal voltage waveform and torque used for the experiments are also used in the 2D finite-element analysis (FEA) model for loss calculations. The losses in the stator winding, stator iron, rotor iron can be obtained through the 2D FEA directly.

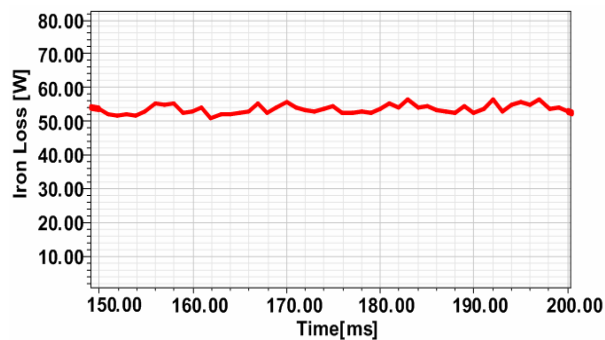
4.2 Thermal simulation

The losses are assigned into individual components of the machine thermal model to estimate the temperature-rise of the machine. In order to develop an accurate thermal model, the conduction, convection, and radiation behaviour within the machine were considered.

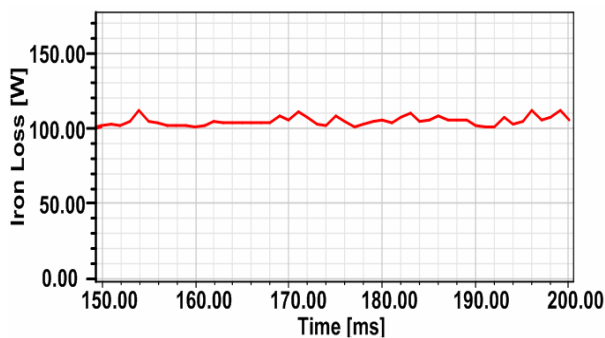
5 Comparison between empirical and simulation results

The simulated iron losses are described in Figure 6 and Figure 7 for sine and PWM supply respectively and concluded in Table 1. The iron loss with load condition is twice the iron loss at no load operation with a sinusoidal supply. When driven by the inverter, the iron loss with a load is 1.5 times greater than the iron loss with no load.

Figure 6 Iron losses from simulation for sine supply, (a) no-load (b) with-load (see online version for colours)



(a)



(b)

Figure 7 PWM losses from simulation, (a) no-load (b) with-load (see online version for colours)

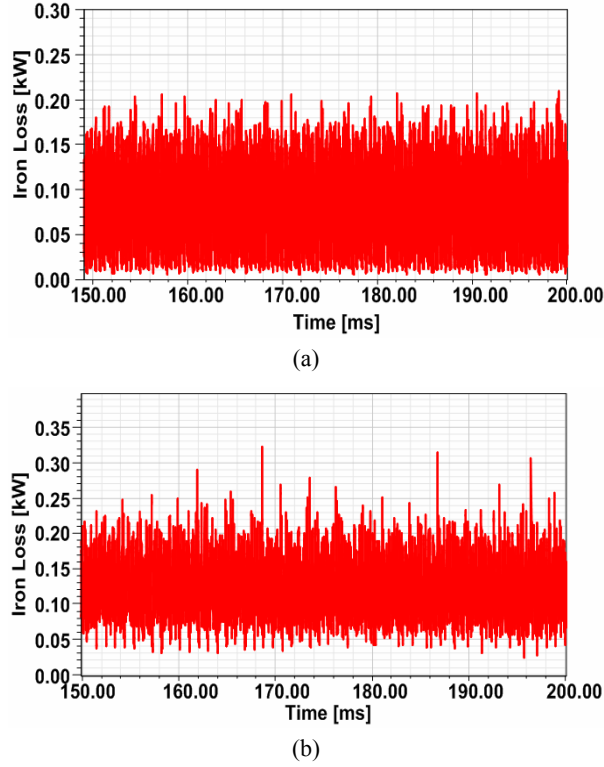


Table 1 Losses from simulation

	<i>No-load (W)</i>		<i>Load (W)</i>	
	<i>PWM</i>	<i>Sine</i>	<i>PWM</i>	<i>Sine</i>
Iron loss	88.5	53.9	130.0	118.6
Copper loss	139.5	50.1	150.1	113.7

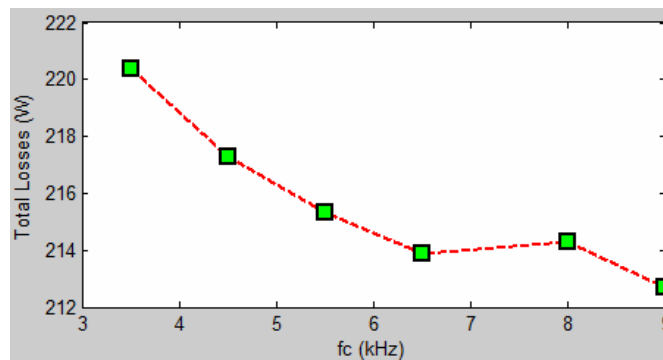
All the losses from experiments are shown in Table 2. Under no load operation, the iron loss with PWM supply is 104 W, a 48.2 W increase over the iron loss when operated from sinusoidal supply (55.8 W). However, when the motor is attached to the load, additional iron losses are induced by the harmonics in the PWM supply, with iron loss at 139.1 W or only 31.1 W more than the sinusoidal iron loss (108 W).

Table 2 Losses from experiments

	<i>No-load (W)</i>		<i>Load (W)</i>	
	<i>PWM</i>	<i>Sine</i>	<i>PWM</i>	<i>Sine</i>
Iron loss	104	55.8	139.1	108
Copper loss	133.7	58.8	148.9	124.5

The test results are consistent with the simulation results at fixed switching frequencies. In order to understand the impact of switching frequency on the additional losses, tests have been conducted using several different switching frequencies (3.5 kHz to 9 kHz) for the PWM inverter. The results are shown in Figure 8. The total losses decrease proportionally with the increase of frequency, which is consistent with prior work (Liu et al., 2008; Khluabwannarat et al., 2007).

Figure 8 Loss with different switching frequencies (see online version for colours)



The 3D FEM thermal model of the motor is developed as shown in Figure 5. Assigning all the losses into the 3D FEM model and setting the necessary boundary conditions, the temperature profile of the motor is obtained after simulation. Figure 9 shows the temperature distribution in stator with no load in sine supply. Table 3 and Table 4 show the entire temperature of the motor from simulation and measurement. Infrared radiation thermometers are used to measure the temperatures at points 1 to 7. The locations of test points are shown in Figure 10 except point 1, which is in the centre of outer surface of housing.

Figure 9 Temperature distribution in stator (see online version for colours)

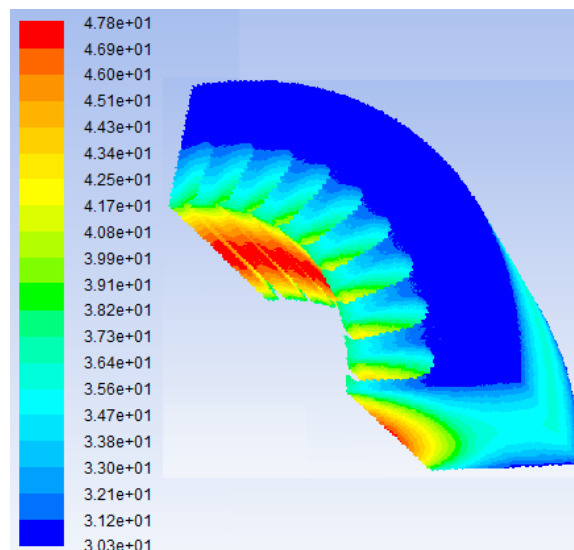


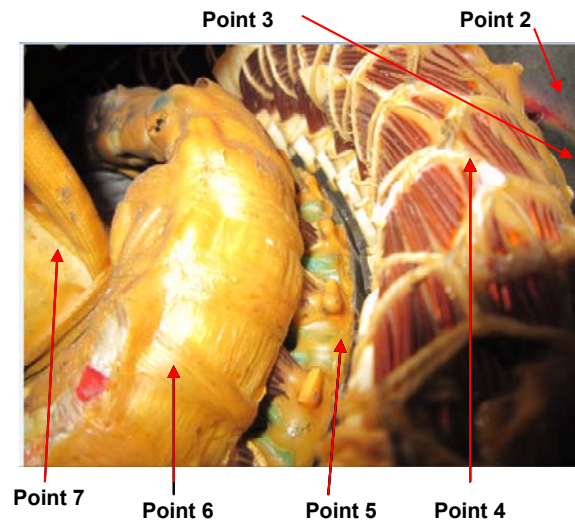
Table 3 Temperature profile with no load

	<i>Experiment (°C)</i>		<i>Simulation (°C)</i>	
	<i>Sine</i>	<i>PWM</i>	<i>Sine</i>	<i>PWM</i>
point 1	31.4	40.9	30.3	37.3
point 2	36.9	42.4	34.7	38.7
point 3	38.2	47.1	35.6	45.6
point 4	39.5	52.7	36.3	49.3
point 5	40.2	51.1	43.3	47.3
point 6	39.6	49.7	34.4	45.4
point 7	50.8	55.7	53.6	53.6

Table 4 Temperature profile with load

	<i>Experiment (°C)</i>		<i>Simulation (°C)</i>	
	<i>Sine</i>	<i>PWM</i>	<i>Sine</i>	<i>PWM</i>
point 1	34.2	41.8	32.7	37.7
point 2	41.4	47.8	37.9	42.9
point 3	47	52.8	44.6	50.6
point 4	50.8	57.2	49.7	53.7
point 5	60.5	63.9	55.5	56.3
point 6	59.9	63.3	52.3	55.3
point 7	67.6	71.7	63.6	66.7

Figure 10 Inside view of the experimental motor (see online version for colours)



It can be seen from Table 3 and Table 4 that the temperature-rise of the induction motor is significantly higher when driven by PWM inverter than driven by sinusoidal power supply. It therefore concludes that for induction motor design, it is important to consider

the additional losses generated due to the harmonics in the PWM supply and possible excessive temperature-rise inside the machine. Extra caution needs to be given to applications which experience wide ambient temperature ranges, such as the ones used in hybrid electric vehicle.

6 Conclusions

In this paper, the impact of an inverter on the losses and thermal characteristics of induction motors has been investigated. The PWM supply induces additional losses, which were manifested as a temperature-rise within the motor. Furthermore, the proportion of losses due to the PWM harmonics experiences a reduction from no load to load operation. The overall losses slightly decrease as higher switching frequencies in the PWM supply are adopted. The temperature-rise due to the additional losses is substantial compared to the machine operated from sinusoidal sources. We hope to provide some guidelines in induction motor design through the investigation of this paper when considering the loss and thermal issues.

Acknowledgements

The authors would like to acknowledge ANSYS Inc. for their support of software (Maxwell, Simplorer, and ePhysics) used in this research. The authors express their gratitude to Madhur Bhattacharya who read the paper.

References

- Adley, K., Cao, W., Clare, J. and Wheeler, P. (2008) 'Predicting inverter-induced harmonic loss by improved harmonic injection', *IEEE Transactions on Power Electronics*, September, Vol. 23, No. 5, pp.2619–2624.
- Benhaddadi, M., Khaldi, R. and Benghanem, M. (1997) 'Experimental study of heating in induction motor fed by PWM inverter', *Proceedings of IEEE Instrumentation and Measurement Technology Conference, 'Sensing, Processing, Networking' IMTC/97*, 19–21 May, Vol. 1, pp.335–338.
- Boglietti, A., Cavagnino, A. and Lazzari, M. (2010) 'Fast method for the iron loss prediction in inverter-fed induction motors', *IEEE Transactions on Industry Applications*, March–April, Vol. 46, No. 2, pp.806–811.
- Boglietti, A., Cavagnino, A., Lazzari, M. and Pastorelli, A. (2002) 'A simplified thermal model for variable speed self cooled industrial induction motor', *37th Industry Applications Conference, IAS Annual Meeting*, Vol. 2, pp.723–730.
- Boglietti, A., Ferraris, P. and Lazzari, M. (1994) 'Power de-rating for inverter fed induction motors', *Conference Record of the 1994 IEEE Industry Applications Society Annual Meeting*, 2–6 October, Vol. 1, pp.55–61.
- Bradley, K., Cao, W., Clare, J. and Wheeler, P. (2008) 'Predicting inverter-induced harmonic loss by improved harmonic injection', *IEEE Transactions on Power Electronics*, September, Vol. 23, No. 5, pp.2619–2624.

- Cao, W., Bradley, K.J., Clare, J.C. and Wheeler, P.W. (2010) 'Comparison of stray load and inverter-induced harmonic losses in induction motors using calorimetric and harmonic injection methods', *IEEE Transactions on Industry Applications*, January–February, Vol. 46, No. 1, pp.249–255.
- Demetriades, G.D., de la Parra, H.Z., Andersson, E. and Olsson, H. (2010) 'A real-time thermal model of a permanent-magnet synchronous motor', *IEEE Transactions on Power Electronics*, February, Vol. 25, No. 2, pp.463–474.
- Halasz, S., Csonka, G., Hassan, A.A.M. and Huu, B.T. (1996) 'Analysis of the unipolar PWM techniques', *8th Mediterranean Electrotechnical Conference, MELECON '96*, 13–16 May, Vol. 1, pp.353–356.
- Karagol, S. and Bikdash, M. (2010) 'Generation of equivalent-circuit models from simulation data of a thermal system', *IEEE Transactions on Power Electronics*, April, Vol. 25, No. 4, pp.820–828.
- Khluabwannarat, P., Thammarat, C., Tadsuan, S. and Bunjongjit, S. (2007) 'An analysis of iron loss supplied by sinusoidal, square wave, bipolar PWM inverter and unipolar PWM inverter', *International Power Engineering Conference, IPEC 2007*, 3–6 December, pp.1185–1190.
- Lee, J-J., Kim, Y-K., Nam, H., Ha, K-H., Hong, J-P. and Hwang, D-H. (2004) 'Loss distribution of three-phase induction motor fed by pulse width-modulated inverter', *IEEE Transactions on Magnetics*, March, Vol. 40, No. 2, pp.762–765.
- Liu, R., Mi, C.C. and Gao, D.W. (2008) 'Modeling of eddy-current loss of electrical machines and transformers operated by pulsewidth-modulated inverters', *IEEE Transactions on Magnetics*, August, Vol. 44, No. 8, pp.2021–2028.
- Mendes, A.M.S., Lopez-Fernandez, X.M. and Cardoso, A.J.M. (2008) 'Thermal performance of a three-phase induction motor under fault tolerant operating strategies', *IEEE Transactions on Power Electronics*, May, Vol. 23, No. 3, pp.1537–1544.
- Park, J-D., Kaley, C. and Hofmann, H.F. (2008) 'Analysis and reduction of time harmonic rotor loss in solid-rotor synchronous reluctance drive', *IEEE Transactions on Power Electronics*, March, Vol. 23, No. 2, pp.985–992.
- Roshen, W.A. (2007) 'A practical, accurate and very general core loss model for nonsinusoidal waveforms', *IEEE Transactions on Power Electronics*, January, Vol. 22, No. 1, pp.30–40.
- Thammarat, C., Tadsuan, S., Suechoey, B. and Bunjongjit, S. (2005) 'The result analysis of the power loss 3-phase induction motor with PWM inverter supply', *The 7th International Power Engineering Conference, IPEC 2005*, 29 November to 2 December, pp.836–841, Vol. 2.
- Uddin, M.N. and Nam, S.W. (2008) 'New online loss-minimization-based control of an induction motor drive', *IEEE Transactions on Power Electronics*, March, Vol. 23, No. 2, pp.926–933.
- Yang, J., Lee, S.B., Yoo, J., Lee, S., Oh, Y. and Choi, C. (2007) 'A stator winding insulation condition monitoring technique for inverter-fed machines', *IEEE Transactions on Power Electronics*, September, Vol. 22, No. 5, pp.2026–2033.